Advances in Enzyme Research, 2015, 3, 75-80
Published Online September 2015 in SciRes. http://www.scirp.org/journal/aer
http://dx.doi.org/10.4236/aer.2015.33008

Subunit Arrangement of a 2-Ketoisovalerate Ferredoxin Oxidoreductase from *Thermococcus profundus* Revealed by a Low Resolution X-Ray Analysis

Yukiko Ozawa[1], Yasufumi Umena[2], Takeo Imai[1], Yukio Morimoto[3*]

[1]Department of Life Science and Graduate School of Life Science, Rikkyo (St. Paul's) University, Tokyo, Japan
[2]Photosynthesis Research Center, Okayama University, Okayama, Japan
[3]Research Reactor Institute, Kyoto University, Osaka, Japan
Email: [*] morimoto@rri.kyoto-u.ac.jp

Received 5 August 2015; accepted 5 September 2015; published 8 September 2015

Abstract

2-ketoisovalerate ferredoxin oxidoreductase (VOR) is a key enzyme in hyperthermophiles catalyzing the coenzyme A-dependent oxidative decarboxylation of aliphatic amino acid-derived 2-keto acids. The enzyme purified under anaerobic conditions from a hyperthermophilic archaeon, *Thermococcus profundus*, is a hetero-octamer $(\alpha\beta\gamma\delta)_2$ consisting of four different subunits, α = 45 kDa, β = 31 kDa, γ = 22 kDa and δ = 13 kDa, respectively, and it has three [4Fe-4S] clusters per $\alpha\beta\gamma\delta$-protomer, similar to other ferredoxin oxidoreductases. In the present study, the native enzyme was purified from this strain and crystallized to give rod-like crystals that were suitable for X-ray diffraction experiments. The crystals belonged to space group $P4_12_12$, with unit-cell parameters $a = b$ = 136.20 Å, c = 221.07 Å. Diffraction images were processed to a resolution of 3.0 Å. The data collected so far indicate the approximate molecular boundaries and a partial main-chain trace of the enzyme.

Keywords

Oxidoreductase, X-Ray Analysis, Iron-Sulfur Cluster

[*]Corresponding author.

How to cite this paper: Ozawa, Y., Umena, Y., Imai, T. and Morimoto, Y. (2015) Subunit Arrangement of a 2-Ketoisovalerate Ferredoxin Oxidoreductase from *Thermococcus profundus* Revealed by a Low Resolution X-Ray Analysis. *Advances in Enzyme Research*, **3**, 75-80. http://dx.doi.org/10.4236/aer.2015.33008

1. Introduction

An energy-producing pathway in the hyperthermophilic archaeon, *Thermococcus profundus*, has been proposed to degrade amino acids [1] [2]. In this pathway, amino acids produced from some peptides by peptidases are converted to their corresponding 2-keto acids by transaminases. The 2-ketoisovalerate ferredoxin oxidoreductase (VOR) catalyzes a reaction to produce acetyl CoA in the presence of coenzyme A from these 2-keto acids through oxidative decarboxylation. Pyruvate ferredoxin oxidoreductase (PFOR) is one of the well-characterized members of the ferredoxin-dependent enzyme family [3]-[5], and it has been shown to catalyze the production of acetaldehyde in the presence of coenzyme A [6]. However, the enzymes indolepyruvate ferredoxin oxidoreductase (IOR) [7], 2-ketoglutarate ferredoxin oxidoreductase (KGOR) [8] and 2-ketoisovalerate ferredoxin oxidoreductase (VOR) [9] are relatively poorly characterized, and their physiological functions have not been established experimentally [10] [11]. Four types of enzyme form a structurally related superfamily in which the enzymes each contain thiamine pyrophosphate, magnesium ions, and one to three [4Fe-4S] cluster(s) as prosthetic groups. The spatial arrangement of the cofactors in *D. africanus* PFOR is clarified by X-ray crystallographic analysis [4], but the three-dimensional structures of the other three types of enzyme are not yet known. In order to investigate the structure-function relationships and deduce specific substrate recognition mechanisms of these four types of enzyme (PFOR, VOR, KGOR, IOR), we report here the purification and crystallization of VOR from *Thermococcus profundus* and a preliminary analysis of crystallographic data collected for this enzyme.

2. Materials and Methods

2.1. Isolation and Purification of Protein

The protein was purified from the native organism, *Thermococcus profundus.* Isolation of the VOR has been described in a previous report [12]. Cell-free extracts were loaded onto a Q-sepharose Fast Flow (GE Healthcare) column equilibrated with buffer. After a wash step the enzyme fraction was eluted with a NaCl linear gradient and then applied onto a hydroxyapatite column followed by a RedTOYOPEALE (TOSOH Bioscience) column. The fractions that contained VOR alone (**Figure 1(a)**) in the buffer of 50 mM Tris-HCl, pH 8, 1 mM thiamine pyrophosphate, 1 mM $MgSO_4$, 0.5 M NaCl, 2 mM dithiothreitol, 2 mM sodium dithionite (SIGMA Aldrich) were concentrated with an Amicon YM50 (Merck Millipore Corporation) membrane, in which the buffer was degassed and purged oxygen by a babbling of Ar gas. Protein concentration was estimated by the method of Bradford [13] modified by use of the rose bengal (Food Red No. 105) [12].

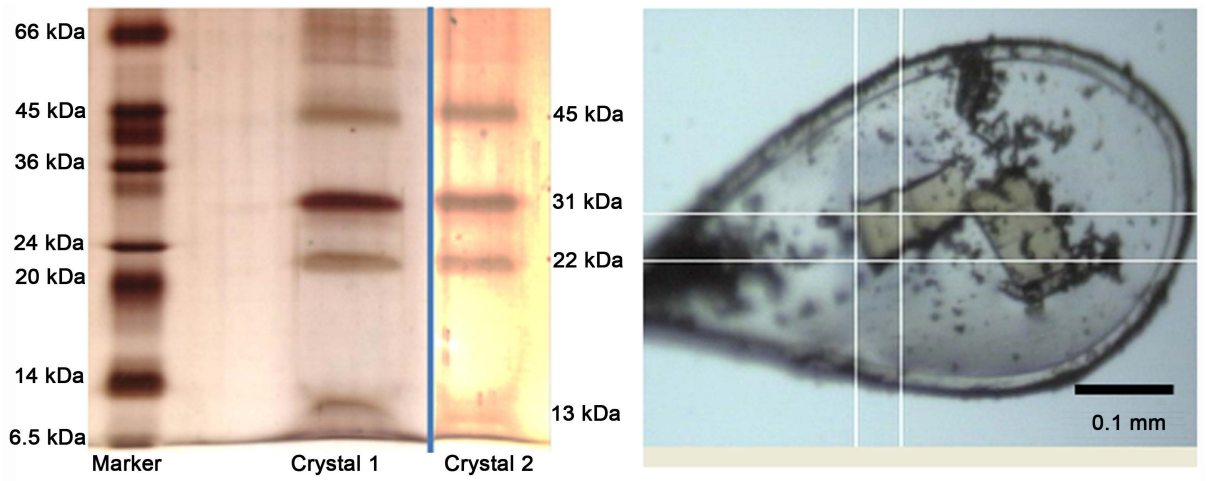

Figure 1. Purity and crystals of VOR. (a) Silver-stained SDS polyacrylamide gels showing the proteins within one dissolved crystal; left lane, molecular weight marker; middle lane, crystal 1; right lane crystal 2 (high contrast). A line is drawn between lanes showing proteins in crystal 1 and crystal 2; (b) Brownish crystals with a few stains caused by protein precipitation in a cryo-loop at the goniometer head. Scale bar is 0.1 mm.

2.2. Crystallization

Crystallization of VOR was carried out using a hanging-drop vapor diffusion method at 293 K under the following condition: 2 µl protein solution concentrated to 10 mg·ml^{-1} was mixed with 2 µl reservoir solution containing 13% (w/v) PEG6000, 0.1 M sodium cacodylate buffer at pH 6.0, 0.1 M $MgCl_2$, 2 mM sodium dithionite, 10 mM dithiothreitol and the droplet was equilibrated against 1 ml reservoir solution (**Table 1**). These crystallization handling was set up in an anaerobic chamber to keep oxygen free with nitrogen gas flow. A few weeks later, crystals appeared and grew to rod-shaped crystals of 0.1 mm length (**Figure 1(b)**).

2.3. Data Collection and Processing

Crystals of VOR were soaked for approximately 20 - 30 sec in a cryoprotectant solution, which was the reservoir solution containing 10% - 20% glycerol. The crystals were mounted and flash-cooled at 100 K. Diffraction data were collected using synchrotron radiation. The diffraction data, however, were not of sufficient quality to proceed under 15% glycerol condition, because of the low resolution (8 Å) and the splitting of diffraction spots. Since crystals treated without a cryoprotectant solution diffracted well to higher resolution (4 Å), data acquisition for a decision of cell parameters was carried out by enclosing the crystal in a quartz capillary with a small amount of the buffer at 288 K. The crystal was analyzed on the BL5A at the Photon Factory (Tsukuba, Japan) and the BL44XU in the Spring-8 (Harima, Japan). After decision of cell parameters and crystal setting, a crystal treated by 20% glycerol protectant and frozen by dipping it into liquid N_2 was used for high and low data acquisition. The crystal-to-detector distance was 800mm for low resolution (116.0 - 5.1 Å) and 500 mm for high resolution (50.0 - 3.0 Å) data, and exposure times were 5 and 3 seconds, respectively. The data were collected from 1 to 180 degrees with an oscillation range of 0.5 degree (low resolution) and 1 degree (high resolution). All diffraction images were processed with the programs iMOSFLM [14] and SCALA [15] of the CCP4 program suite [16]. All data from high and low resolution data sets were merged and scaled to one data set up to 3 Å resolution. The statistics of data collection and processing are summarized in **Table 2** and **Table 3**.

Table 1. Crystallization condition and details.

Method	Vapor diffusion
Plate type	Hanging-drop 24 wells
Temperature (K)	293 K
Protein concentration	10 mg/ml
Buffer composition of protein solution	50 mM Tris-HCl (pH 8.0)/0.2 M NaCl/4 mM DTT
Composition of reservoir solution	13% (w/v) PEG6000, 0.1 M sodium cacodylate buffer at pH 6.0, 0.1 M $MgCl_2$, 2 mM sodium dithionite, 10 mM dithiothreitol
Volume and ratio of drop	4 µl 1:1
Volume of reservoir	1 ml

Table 2. Crystallographic data and collection.

Space group	$P4_12_12$
Cell dimensions	
a, *b*, *c* (Å)	136.20, 136.20, 221.07
α, *β*, *γ* (˚)	90.00, 90.00, 90.00
Resolution (Å)	3.00 (3.16 - 3.00)[a]
R_{merge}	0.075 (0.875)
$I/\sigma I$	5.0 (0.5)
Completeness (%)	100.0 (99.9)
Redundancy	3.6 (2.6)

[a]Values in parentheses are for the highest-resolution shell.

Table 3. Refinement statistics.

Resolution (Å)	116.0 - 3.00
No. reflections	40,114
R_{work}[b]/R_{free}[c]	0.3196/0.3674
No. atoms	
Protein	7158
Ligand/ion	0
Water	0
B-factors	
Protein	104.77
R.m.s. deviations	
Bond lengths (Å)	0.170
Bond angles (˚)	2.674

[b]R_{work} was calculated from the working set (95% of the data). [c]R_{free} was calculated from the test set (5% of the data).

3. Results and Discussion

The VOR crystal is a rectangular prism, crystallizing in a tetragonal crystal group with unit-cell parameters: a = b = 136.20 Å, c = 221.07 Å. The space group, however, is uncertain because the reflection data characterizing the extinctions along the a^* = b^* and c^* axes are not recorded. A silver stained SDS electrophoresis gel of one dissolved crystal clearly showed four bands demonstrating that all four subunits were present in the crystal (**Figure 1(a)**). The calculated molecular weight of the VOR $\alpha\beta\gamma\delta$-protomer is 111 kDa, and the Matthews coefficient (V_M) [17] is calculated to be 2.2 $Å^3Da^{-1}$ for sixteen molecules per unit cell. A self-rotation function calculated using low resolution data (4 Å) from the *P*1 space group shows definite peaks at each of the *a*-, *b*-, and *c*-axes and a diagonal position between *a*- and *b*- for a 2-fold symmetry with kappa = 180˚, and also one peak along the *c*-axis for a 4-fold symmetry with kappa = 90˚. From these results, we have concluded that the crystal corresponds to the 4/mmm Laue group and two $\alpha\beta\gamma\delta$-protomers exist in each asymmetric unit.

Although the amino acid sequence of the VOR from *T. profundus* has not been determined, the sequence of a homologous enzyme, VOR from *P. furiosus*, has been determined and amino acid identities are 29% (*pf*VOR: 299 - 664), 33% (792 - 990), 23% (2 - 288) (**Figure 2** upper) and 27% (699 - 747) (**Figure 2** lower) against the PFOR (PDB entry 1b0p, [4]) from *D. africanus*. We tried to solve main-chain structures of the VOR; the PFOR was used as a model molecule for a preliminary structural analysis. A main-chain model created from the PFOR coordinates by deleting side-chain atoms of its amino acids is available for use in a molecular replacement method (MOLREP [18]), and searches of the unit cell are carried out using this model for several related space groups. A proper solution was obtained for the space group $P4_12_12$ with values of 0.234 (Score) and 2.038 (Contrast). A preliminary structural analysis has been carried out using the program *Phenix* [19] and employing this space group and the PFOR main-chain model. PFOR consists of a single polypeptide chain composed of 1232 amino acids, and it appears to have four segments likely to be four domains (PFOR: 2 - 416; *pf*VOR: α-subunit, 417 - 630: δ, 631 - 786: γ, 787 - 1179: β) from its N- to C-terminus. The VOR structure, which is composed of four subunits (α, β, γ, δ, **Figure 1(a)**), is modified by rigid-body refinement and auto-model building using the *Phenix* program, with initial phases obtained from the low resolution data, producing an electron density map showing boundaries of the VOR molecule in the unit cell and assigning four subunits (**Figure 3**). However, the secondary structures of the chain were not yet well defined. The current *R*-factor and R_{free} are 0.3196 and 0.3674 (**Table 3**), respectively. Searches for positions of the iron-sulfur clusters in the δ and β-subunits corresponding to the PFOR structure and of the other protomer in an asymmetric unit, and modifications of the VOR model corresponding to molecular weight of each subunit using a solvent-flattening method to improve the initial phases, are currently in progress.

```
pfVOR   2    IEIRFHGRGGQGAVTAANILASAAFKEGK--YVQAFPFFGVERRGAPVTAFTRIDNKPIR  59
PFOR    417  IQCQFWGLGADGTV-GANKQAIKIIGDNTDLFAQGYFSYDSKKSGGITISHLRFGEKPIQ  475

pfVOR   60   IKTQIYEPDVVVVLDPSLLDAVDVTAGLKDEGIVIVNTEKSKEEVLEK---------LKK  110
PFOR    476  STYLVNRADYVACHNPAYVGIYDILEGIKDGGTFVLNSPWSSLEDMDKHLPSGIKRTIAN  535

pfVOR   111  KPKKLAIVDATTIALEI-LGLPITNTAILGAVAKATGLVKIESIEEAIKDTFS---GELG  166
PFOR    536  KKLKFYNIDAVKIATDVGLGGRI-NMIMQTAFFKLAGVLPFEKAVDLLKKSIHKAYGKKG  594

pfVOR   167  EK----NARAAREAYEKTEVFE----------------LMNTLFGKTKEEAKPIVLKSVD  206
PFOR    595  EKIVKMNTDAVDQAVTSLQEFKYPDSWKDAPAETKAEPMTNEFF---KNVVKPILTQQGD  651

pfVOR   207  EYP------EAPISLGTTLVNPTGDWRTFKPVVNEEKCVKCYICWKYCPEPAIYI-----  255
PFOR    652  KLPVSAFEADGRFPLGTSQFEKRGVAINV-PQWVPENCIQCNQCAFVCPHSAILPVLAKE  710

pfVOR   256  -----KPDGYVAID--------YDY--------CKGCGICANECPTKAITMIKE  288
PFOR    711  EELVGAPANFTALEAKGKELKGYKFRIQINTLDCMGCGNCADICPPKEKALVMQ  764

pfVOR   699  FEEHFYAGHTACQGCGASLGLRYVLKAYGKKTILVIPACCSTIIAGPWP  747
PFOR    800  FQEPLMEFSGACSGCGETPYVRVITQLFGERMFIANATGCSSIWGASAP  848
```

Figure 2. Amino acid alignment of the *pf*VOR and PFOR. Cys bound Fe atoms are bold. Upper: *pf*VOR $\gamma\delta$-subunit, lower: a part of β-subunit.

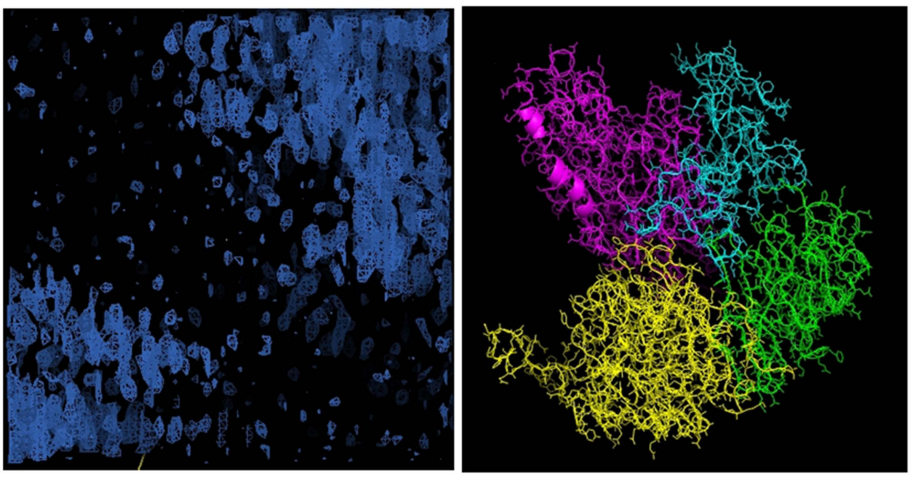

(a) (b)

Figure 3. Electron density maps of the VOR structure at 3 Å resolution; (a) boundaries of the enzyme molecules, (b) subunit arrangement of the enzyme (α-subunit: yellow, β: magenta, γ: cyan, δ: green).

Acknowledgements

This work was supported by a Grants-in-Aid for Scientific Research (22570113(YM)) from the Ministry of Education, Science and Culture of Japan and the Customer Care Plan Foundation (YM), and by a Project Research Program under approvals 25P6-1 and 23P2-5 of Research Reactor Institute, Kyoto University. The synchrotron radiation experiments were conducted under the approvals 2006AB1422 and 2011AB6647 of SPring-8 and 2006G180 of PF.

References

[1] Ma, K., Loessner, H.J., Heider, J., Johnson, M.K. and Adams, M.W.W. (1995) Effects of Elemental Sulfur on the Metabolism of the Deep-Sea Hyperthermophilic Archaeon Thermococcus Strain ES-1: Characterization of a Sulfur-Regulated, Non-Heme Iron Alcohol Dehydrogenase. *Journal of Bacteriology*, **177**, 4748-4756.

[2] Heider, J., Ma, K. and Adamas, M.W.W. (1995) Purification, Characterization, and Metabolic Function of Tungsten-Containing Aldehyde Ferredoxin Oxidoreductase from the Hyperthermophilic and Proteolytic Archaeon Thermococcus Strain ES-1. *Journal of Bacteriology*, **177**, 4757-4764.

[3] Adams, M.W.W. and Kletzin, A. (1996) In: Adams, M.W.W., Ed., *Advances in Protein Chemistry*, Vol. 48, Academic

Press, New York, 101-180.

[4] Chabriere, E., Charon, M.-H., Volbeda, A., Pieulle, L., Hatchikian, E.C. and Fontecilla-Camps, J.C. (1999) Crystal Structures of the Key Anaerobic Enzyme Pyruvate: Ferredoxin Oxidoreductase, Free and in Complex with Pyruvate. *Nature Structural Biology*, **6**, 182-189. http://dx.doi.org/10.1038/5870

[5] Ragsdale, S.W. (2003) Pyruvate Ferredoxin Oxidoreductase and Its Radical Intermediate. *Chemical Reviews*, **103**, 2333-2346. http://dx.doi.org/10.1021/cr020423e

[6] Ma, K., Hutchins, A., Sung, S.J. and Adams, M.W.W. (1997) Pyruvate Ferredoxin Oxidoreductase from the Hyperthermophilic Archaeon, *Pyrococcus furiosus*, Functions as a CoA-Dependent Pyruvate Decarboxylase. *Proceedings of the National Academy of Sciences of the United States of America*, **94**, 9608-9613. http://dx.doi.org/10.1073/pnas.94.18.9608

[7] Mai, X. and Adams, M.W.W. (1994) Indolepyruvate Ferredoxin Oxidoreductase from the Hyperthermophilic Archaeon *Pyrococcus furiosus*. A New Enzyme Involved in Peptide Fermentation. *Journal of Biological Chemistry*, **269**, 16726-16732.

[8] Mai, X. and Adams, M.W.W. (1996) Characterization of a Fourth Type of 2-Keto Acid-Oxidizing Enzyme from a Hyperthermophilic Archaeon: 2-Ketoglutarate Ferredoxin Oxidoreductase from *Thermococcus litoralis*. *Journal of Bacteriology*, **178**, 5890-5896.

[9] Heider, J., Mai, X. and Adams, M.W.W. (1996) Characterization of 2-Ketoisovalerate Ferredoxin Oxidoreductase, a New and Reversible Coenzyme A-Dependent Enzyme Involved in Peptide Fermentation by Hyperthermophilic Archaea. *Journal of Bacteriology*, **178**, 780-787.

[10] Tersteegen, A., Linder, D., Thauer, R. and Hedderich, R. (1997) Structures and Functions of Four Anabolic 2-Oxoacid Oxidoreductases in Methanobacterium Thermoautotrophicum. *European Journal of Biochemistry*, **244**, 862-868. http://dx.doi.org/10.1111/j.1432-1033.1997.00862.x

[11] Siddiqui, M.A., Fujiwara, S. and Imanaka, T. (1997) Indolepyruvate Ferredoxin Oxidoreductase from *Pyrococcus* ap. KOD1 Possesses a Mosaic Structure Showing Features of Various Oxidoreductases. *Molecular and General Genetics*, **254**, 433-439.

[12] Ozawa, Y., Nakamura, T., Kamata, N., Yasujima, D., Urushiyama, A., Yamakura, F., Ohmori, D. and Imai, T. (2005) *Thermococcus profundus* 2-Ketoisovalerate Ferredoxin Oxidoreductase, a Key Enzyme in the Archaeal Energy-Producing Amino Acid Metabolic Pathway. *The Journal of Biochemistry*, **137**, 101-107. http://dx.doi.org/10.1093/jb/mvi012

[13] Bradford, M.M. (1976) A Rapid and Sensitive Method for the Quantitation of Microgram Quantities of Protein Utilizing the Principle of Protein-Dye Binding. *Analytical Biochemistry*, **72**, 248-254. http://dx.doi.org/10.1016/0003-2697(76)90527-3

[14] Battye, T.G.G., Kontogiannis, L., Johnson, O., Powell, H.R. and Leslie, A.G.W. (2011) *iMOSFLM*: A New Graphical Interface for Diffraction-Image Processing with *MOSFLM*. *Acta Crystallographica*, **D67**, 271-281. http://dx.doi.org/10.1107/s0907444910048675

[15] Evans, P. (2006) Scaling and Assessment of Data Quality. *Acta Crystallographica*, **D62**, 72-82. http://dx.doi.org/10.1107/s0907444905036693

[16] Potterton, E., Briggs, P., Turkenburg, M. and Dodson, E. (2003) A Graphical User Interface to the *CCP*4 Program Suite. *Acta Crystallographica*, D**59**, 1131-1137. http://dx.doi.org/10.1107/S0907444903008126

[17] Matthews, B.W. (1968) Solvent Content of Protein Crystals. *Journal of Molecular Biology*, **33**, 491-497. http://dx.doi.org/10.1016/0022-2836(68)90205-2

[18] Vagin, A. and Teplyakov, A. (2010) Molecular Replacement with *MOLREP*. *Acta Crystallographica*, D**66**, 22-25. http://dx.doi.org/10.1107/S0907444909042589

[19] Adams, P.D., Afonine, P.V., Bunkóczi, G., Chen, V.B., Davis, I.W., Echols, N., Headd, J.J., Hung, L.-W., Kapral, G.J., Grosse-Kunstleve, R.W., McCoy, A.J., Moriarty, N.W., Oeffner, R., Read, R.J., Richardson, D.C., Richardson, J.S., Terwilliger, T.C. and Zwart, P.H. (2010) *PHENIX*: A Comprehensive Python-Based System for Macromolecular Structure Solution. *Acta Crystallographica*, **D66**, 213-221. http://dx.doi.org/10.1107/s0907444909052925